NACA

RESEARCH MEMORANDUM

INVESTIGATION OF OPERATING PRESSURE RATIO OF A SUPERSONIC WIND TUNNEL UTILIZING DISTRIBUTED BOUNDARY-LAYER SUCTION IN TEST SECTION

By C. B. Cohen and A. S. Valerino

Lewis Flight Propulsion Laboratory
Cleveland, Ohio

NATIONAL ADVISORY COMMITTEE FOR AERONAUTICS

WASHINGTON
November 1, 1950

NATIONAL ADVISORY COMMITTEE FOR AERONAUTICS

RESEARCH MEMORANDUM

INVESTIGATION OF OPERATING PRESSURE RATIO OF A SUPERSONIC WIND TUNNEL UTILIZING DISTRIBUTED BOUNDARY-LAYER SUCTION IN TEST SECTION

By C. B. Cohen and A. S. Valerino

SUMMARY

An investigation to determine the effect of distributed boundary-layer suction on the pressure recovery of a supersonic wind tunnel has been conducted in a 3.84- by 10-inch tunnel operating at a Mach number of 2.0. With suction applied to two walls of a constant-area section in the vicinity of the normal shock, a reduction of 4 percent of the operating pressure ratio was obtained. This reduction was attributed to an improvement (reduction in Mach number) in the flow characteristics at the subsonic-diffuser inlet.

The normal shock predicted by one-dimensional theory was, in practice, replaced by a multiple-branch shock configuration. The change in static pressure, total pressure, and Mach number occurred gradually in the streamwise direction and finally approached the predicted Rankine-Hugoniot values.

INTRODUCTION

The high operating power requirements currently associated with supersonic wind tunnels are primarily the result of the irreversible processes encountered in diffusion. The total-pressure losses associated with these irreversibilities may be divided into shock losses and viscous losses. Many methods of decreasing the shock losses by lowering the supersonic Mach number at which the terminal shock occurs have been investigated. In practice, however, the losses incurred by the operation of a supersonic tunnel with the shock at a given Mach number have, in general, been found to be considerably above those theoretically predictable. Neumann and Lustwerk (reference 1) have shown these excessive losses to be associated with the flow separation behind the shock, and have found that a long constant-area section downstream of the shock allows the flow to reattach itself to the walls and results in pressure recoveries very near the theoretical value.

An investigation was conducted at the NACA Lewis laboratory to determine the merit of continuous suction on two walls of a constant-area extension of the test section, immediately preceding the subsonic diffuser of a supersonic wind tunnel, primarily as a means of reducing the separation losses and hence the operating power requirements. A secondary purpose was to study the stability and the form of the terminal shock-wave configuration by means of high-speed schlieren photographs. The research was conducted at a Mach number of 2.0 in a 3.84- by 10-inch supersonic wind tunnel operating with a test section 46 inches long. Boundary-layer removal was accomplished by suction through compartmented walls covered with a smooth-surface screen.

In order to approach an optimum bleed configuration, further development of boundary-layer suction was attempted by utilizing complete peripheral suction. The screen installation was destroyed, however, before sufficient data were obtained.

APPARATUS AND PROCEDURE

The investigation was conducted in the NACA Lewis 3.84- by 10-inch supersonic wind tunnel operating at a Mach number of 2.0 and at a Reynolds number of approximately 5×10^6 per foot (fig. 1). The nozzle from throat to test section was 38.4 inches long. Behind the nozzle was a constant-area section 46 inches in length and a subsonic diffuser 139 inches in length with a rectangular cross section. The horizontal walls of the diffuser diverged at an angle of 5° and the vertical walls diverged at an angle of 6°.

The porous walls (fig. 2) were each 30 inches long and 3.84 inches wide and were divided into fifteen 2-inch compartments. These compartments were covered by a steel grill to which was soldered a 40-mesh electroplated copper-nickel screen (18-percent open area) with its smooth surface outward.

Static-pressure orifices were provided along the surface of the nozzle, along the 3.84-inch walls of the tunnel, and in the partitions between the suction compartments (fig. 2). Total pressures were measured by two 12-tube rakes at the inlet (station 3) and outlet (station 4) of the subsonic diffuser. A static-pressure tube located on the tunnel center line was included in the rake at station 3. Total pressures were calculated by numerical integration of the 12 individual tube readings. The distribution of weight-flow removal was determined by a single pitot-static probe in each

of the thirty 1-inch tubes leading from the suction compartments to common manifolds. The absolute magnitude of the weight flow removal was then corrected by use of two 10-tube rakes located in a region of well-developed flow in 4-inch-diameter pipes leading from the suction manifolds.

All pressures were photographically recorded on multiple-tube manometers using dibutylphthalate (S.G. ≈1.0) as the indicating fluid for the suction manifold rakes and mercury for the remaining tubes. Air-flow conditions in the constant-area section were observed with a two-mirror schlieren system and were photographed using 4-microsecond exposures. High-speed schlieren motion pictures were also taken occasionally with a Western Electric Fastex camera to observe the shock motion.

Air with a specific humidity of approximately 0.0002 entered the tunnel settling chamber at a pressure of 41 inches of mercury absolute and a temperature of 80° F. The tunnel outlet was connected to a bank of reciprocating exhausters, which also furnished the suction for the boundary layer.

For each run, after inlet conditions were established, the tunnel outlet valve was so adjusted that the terminal shock-wave was located in the subsonic diffuser. The pincher valves (fig. 1) were then set by reference to a mercury manometer to give an approximately uniform distribution of boundary-layer removal along the 3.84 inch walls. For the remainder of the run, the tunnel outlet valve setting was varied to move the terminal shock configuration through the constant-area section of the tunnel. Manometer and schlieren photographs were taken at each position. For succeeding runs, the uniform distribution of boundary-layer removal was maintained as the mass flow bled was increased. The aforementioned procedure was then repeated.

The symbols used herein are defined in appendix A.

RESULTS AND DISCUSSION

Comparison of the original tunnel pressure ratios (no screen installed) with those obtained from the tunnel including the screen installation but with no applied suction is presented in figure 3 as a function of the shock position l/h. The total-pressure ratio to the subsonic diffuser inlet P_0/P_3 was essentially unchanged by the addition of the screen. The operating-pressure ratio P_0/P_4, however, increased 2 to 4 percent by using the screen installation

with no suction. This increase is indicative of the penalties on the required starting-pressure ratio when no suction is applied to such a screen installation incorporated in a tunnel.

The large difference in total-pressure ratios between station 3 and 4 indicated flow separation in the subsonic diffuser. This difference decreased with an increase in the length of run between the shock and the subsonic diffuser. This trend is in agreement with the results of reference 1, where pressure ratios near theoretical were obtained in constant-area round pipes at a test-section Mach number of 2.0 with a distance from the shock to the subsonic diffuser inlet that was approximately 10 diameters. Thus the performance of the subsonic diffuser is largely dependent on the condition of its entering flow.

Data from a typical reading with suction applied are shown in figure 4. For each reading the pressure distribution, the weight-flow removal distribution and the pressure recovery at stations 3 and 4 were determined.

The shock-wave configuration appeared as a blurred branch shock when viewed on the ground glass screen. High-speed schlieren photographs, however, revealed a multiple-branch shock as shown in the sketch in figure 4. In general, the pressure rise on the wall was apparent 2 to 4 inches upstream of the free-stream shock wave as observed with the schlieren apparatus. This trend was probably due to the interaction effects between the initial shock wave and the boundary layer. The static-pressure distribution on the wall always showed a pressure rise starting steeply and then gradually decreasing in slope. The entire static-pressure rise was less than indicated by a theoretical normal shock at the free-stream Mach number. As would be expected, the bleedoff-distribution curve followed closely the shape of the pressure-distribution curve.

If suction were applied to flow configurations with severe boundary-layer separation, it is expected that the boundary-layer would be pulled toward the walls, thus diminishing the extent of the separation and consequently decreasing the over-all required pressure ratio. The data for a typical run shown in figure 5 include the variation with shock position of P_0/P_4 and P_0/P_3. When the shock was moved upstream, P_0/P_4 decreased rapidly and the bleed weight-flow ratio W_b/W_t increased. The mean value of P_0/P_3 was about 10 percent above the theoretical normal shock value.

A summary of the effect of the boundary-layer suction on the over-all required pressure ratio is shown in figure 6(a) by cross plots of curves for each run (similar to figs. 3 and 5). The pressure ratios P_0/P_4 and P_0/P_3 are plotted as a function of W_b/W_t for several values of l/h. The cross-plotted points are shown for a value of l/h of 2.0 to indicate the magnitude of scatter.

The data shown in this report pertain to the case of a weight-flow removal distribution adjusted as mentioned under APPARATUS AND PROCEDURE. It was found that the bleedoff farthest downstream could be appreciably reduced without noticeably affecting the tunnel operating pressure ratio. Further refinement of bleed distribution may therefore lead to greater power savings.

As previously mentioned, the installation of the screen caused the value of P_0/P_4 to increase for $W_b/W_T = 0$. This increase is shown by the rise in P_0/P_4 from the square symbols to the faired curves for each value of l/h in figure 6(a). Presumably, the extent of this initial increase could be affected by the smoothness and percent open area of the screen used. For this investigation, however, these parameters were held constant. After the initial increase in pressure ratio, the application of bleedoff produced a drop in pressure ratio below the original value, thus yielding a net gain. (The dashed portion of the curve represents the probable trend between zero suction and the lowest value of W_b/W_T investigated.) When the suction was mostly upstream of the shock (for example, $l/h = 2.0$) a point was reached at which the pressure ratio began to increase again. This reversal could be attributed to an effective area increase created by the suction ahead of the shock wave. Apparently, at this point the effect of the expansion exceeded the beneficial reattachment effect behind the shock. In agreement with this hypothesis, the value of W_b/W_T at which the upward trend occurred increased with increasing l/h (decreasing supersonic suction area) until at $l/h = 4.5$ the maximum value of W_b/W_T available with this equipment produced no reversal.

The variation of P_0/P_3 with W_b/W_T is also shown in figure 6(a). The upward trend of P_0/P_4 (at high values of W_b/W_T) for l/h of 2.0 and 2.5 was of such magnitude that it might be completely accounted for by the corresponding increase in P_0/P_3, and tends to confirm that the effect was due to a supersonic expansion. In general, the shape of the P_0/P_3 curves is not

clearly understood; however, the variation of magnitude in each case was always less than ±0.03 from a mean value. Essentially then, most of the savings due to the suction were apparent at station 4 and not at station 3. These gains will be discussed in detail subsequently.

The percentage saving in pressure ratio P_0/P_4 is shown as a function of l/h in figure 6(b). The gains decreased (approximately linearly) with increasing settling length l/h. From this variation it would appear that for a sufficiently great value of l/h no saving would result from the application of suction. A reasonable hypothesis for this length would be the length necessary for natural reattachment as mentioned in reference 1.

A reduction in required pressure ratio of a supersonic tunnel is desirable because of the associated decrease in compressor (or exhauster) pressure ratio and the resultant savings in power requirements. When a decrease in pressure ratio is accomplished by means of a suction installation, however, the power requirements of such an installation may offset any power gains due to pressure ratio. It is thus of interest to compare the pressure-ratio gains shown in figure 6 in terms of total power requirements including bleed-off power. A power factor K (derived in appendix B) is used for this purpose; K is defined as the ratio of calculated total power (including bleed-off) to theoretical normal-shock power.

The variation of this total power factor with weight-flow bleed-off for the six shock positions previously discussed is shown in figure 7(a). The horizontal line for each position represents the power requirements of the original tunnel. For a given shock position, the power began to decrease with increasing bleedoff but reached a minimum value before the corresponding pressure ratio was minimized. The power then increased at approximately the same rate at which it had decreased. As l/h was increased the net power savings became smaller, until at about $l/h = 4.0$ where no saving was realized.

A breakdown of the power requirements for l/h of 2.5 is presented in figure 7(b). The general shape of the curves does not vary significantly from one shock position to another. The upper curve is the same as that for $l/h = 2.5$ in figure 7(a), which shows very little total power saving. For all shock positions the power required for the bleed process increased linearly with W_b/W_T, as would be expected. The internal power curve represents the total power required minus the bleed power. It is noted that at the optimum condition the internal-flow power required has been reduced

approximately 8.5 percent. Thus a significant gain in the primary compressor or exhauster power requirements may be attained if a limited power supply is available for a given tunnel installation. The lowest curve in figure 7(b) shows the power required for the flow to the subsonic-diffuser inlet (station 3). The greatest variation in power required (and hence absorbed) therefore must have occurred in the subsonic diffuser. The power reduction caused by the bleed is of the order of 50 percent and may appear slightly paradoxical inasmuch as no suction was applied in the subsonic diffuser. This result suggests that the improvement is due to a change in the nature of the flow entering the subsonic diffuser.

The most direct evidences of changed inlet-flow conditions are the schlieren pictures of the terminal-shock form with and without boundary-layer suction shown in figure 8. The vertical lines across the photographs are wires strung outside the tunnel to locate the junctures of the suction compartments (every 2 inches) along the 4-inch walls. The numbers identify the various compartments starting with number 1 as the farthest upstream. Figures 8(a), 8(b), and 8(c) show the shock for the range of l/h investigated with the flow direction from right to left. Because the schlieren knife-edge was horizontal, the boundary layer appears as a darkened region at the top and a light region at the bottom of the photographs. The boundary-layer separation and thickness are shown to be considerably reduced by the action of suction. The shock wave appears as a multiple-branch shock configuration, with the branching diminishing appreciably with suction. Four multiple shocks can be seen in some of the photographs and as many as seven have been observed. Proceeding downstream each shock appears to deteriorate somewhat from the preceding one. This deterioration is most noticeable with suction applied. Figure 8(d) shows the effect of schlieren knife-edge orientation. The shock position is the same as in figure 8(b) with suction applied, but the knife-edge has been rotated to a vertical position. Some weak shocks originating from the junctions of suction compartments are visible in figures 8(b) and 8(c).

Because the presence of multiple shock-waves in the channel only requires that the flow be supersonic immediately upstream of each shock, it does not necessarily define the Mach number of the flow in the entire region between the shocks. Thus there is the possibility of a subsonic intermediate region with a re-expansion to supersonic flow. If the latter were the case, the shock waves would each conform with the one-dimensional normal shock concept. However, the observation of bow waves in front of a blunt body placed

throughout the region between shocks denies this possibility and suggests a shock structure of a variety other than normal shocks. The location of the bow wave with respect to the body indicated that the Mach number between the multiple shocks decreased in the stream direction. The fact that the wall static-pressure rise per "section" of this shock configuration (fig. 4) is much less than that for a theoretical normal shock also tends to corroborate this hypothesis. Additional evidence of the weakness of the individual shocks is supplied by the fact that the over-all total-pressure loss through the group of shocks is only slightly greater than a theoretical free-stream normal shock (figs. 3 and 5). Further understanding of this type of shock configuration will depend, however, on a total and static pressure probing of several experimental configurations.

High-speed schlieren motion pictures showed that for the case of the unaltered tunnel the shock configuration became very unstable in the constant-area section. The configuration would oscillate as a unit in the upstream-downstream direction with an amplitude up to 10 inches and with an unconstant frequency. Upon installation of the screen but with no applied suction, the instability was increased, especially in the region of the upstream end of the suction wall. For this condition the amplitude was sometimes as great as 15 inches. With optimum bleedoff the amplitude of the oscillation was greatly reduced, being from 1 to 2 inches at the downstream end of the suction wall and 4 to 6 inches at the upstream end.

The evidence indicated by the schlieren of altered inlet conditions for the subsonic diffuser is also shown by measured total-pressure profiles such as those in figures 9(a), 9(b), and 9(c) for the same values of l/h shown in figure 8. The effective subsonic-diffuser inlet Mach number M_e, which is also tabulated in figure 9, was calculated from the integrated total pressure and an average of a wall and a center line static pressure. Presuming that the significance of a profile depends on the portion of the perimeter of the duct it affects, the profile across the 3.84-inch dimension of the tunnel is the more important because it represents 72.3 percent of the perimeter of the tunnel. The general trends shown in figure 9 are: (1) Installation of the screen with no applied suction created a more peaked profile, which could be associated with greater mixing losses; at the same time the inlet Mach number was, in general, slightly increased. (2) With commencement of suction the profiles flattened and the inlet Mach number decreased with increasing bleed-off.

The variation of profile and M_e was apparently producing the great change in subsonic diffuser losses previously shown. In order to determine which of these variables created the most effect, it was necessary to isolate one. A method of doing this was to plot the effect (subsonic diffuser pressure recovery) as a function of the variable M_e, as shown in figure 10. Curve A is the locus of test points for the original unaltered tunnel and for the tunnel with screen installed and suction applied. For these conditions a variety of profiles was observed. Inasmuch as the points fall nearly on one curve when plotted as a function of Mach number, it may be concluded that for these conditions the variation of M_e was primarily responsible for the variation of P_4/P_3. For the case with the screen installed but no applied suction (curve B), the points fall below curve A. For this case, therefore, the profile was sufficiently unfavorable to reduce the pressure recovery at a given value of M_e. Inasmuch as no extremely low values of W_b/W_T were investigated, few intermediate points between curves A and B were obtained. (See dotted portions of curves in fig. 6(a).) Primarily then, figure 10 indicates that unless the profile of the entry flow is highly unfavorable any change in subsonic diffuser pressure recovery due to suction upstream is largely the effect of a change in inlet Mach number.

The tabulation of M_e in figure 9 also indicates that with no bleed the inlet Mach number can be appreciably reduced by allowing some constant-area length behind the shock before the subsonic diffuser. This trend is more easily seen in figure 11, where M_e is plotted as a function of l/h for the original tunnel and for the altered tunnel with approximately optimum bleed-off (near minimum pressure ratio). The curve for the altered tunnel is an indication of the amount of length that may be replaced by suction for equivalent inlet Mach numbers for this configuration. The upper curve also shows the variation of effective Mach number behind the shock in the constant-area section. With sufficient length, the Mach number is shown to approximately attain the theoretical normal shock value. The dashed portion of the curve indicates the trend obtained from the previously mentioned bow-wave observation.

SUMMARY OF RESULTS

1. In a constant-area channel operating at a test-section Mach number of 2.0, the normal shock predicted by theory did not materialize. Instead, there was a multiple-branch shock configuration

accompanied by boundary-layer separation and a gradual static pressure rise on the wall. The structure of the shock configuration is not clearly understood, but observation of schlieren pictures of the flow indicated that the velocity was supersonic in the regions between the multiple shocks and decreased in the downstream direction. Associated with this configuration of shocks and boundary-layer separation was a high degree of instability indicated by a streamwise oscillation. With no suction applied the amplitude was occasionally observed to be as great as 10 inches. With optimum bleedoff, this amplitude was generally decreased to less than 6 inches and occasionally to less than 2 inches.

2. With sufficient constant-area settling length behind the normal shock to permit flow reattachment, the changes in static pressure, total pressure, and Mach number approached those predicted by theoretical one-dimensional normal shock values.

3. Boundary-layer suction in a constant-area section decreased the severity of separation and the Mach number behind the shock configuration and consequently resulted in an improvement of pressure ratio. In a 3.84- by 10-inch tunnel operating at a test-section Mach number of 2.0, a reduction of operating pressure ratio of greater than 4 percent was observed with $2\frac{1}{2}$ percent bleedoff from the 3.84-inch walls.

4. In general, the reduction in operating pressure ratio was primarily accomplished by the reduction of the Mach number at the subsonic-diffuser inlet. The associated change in total-pressure profile may also have improved the pressure recovery, but unless the profile was highly unfavorable the effect of changing it appeared relatively small.

Lewis Flight Propulsion Laboratory,
National Advisory Committee for Aeronautics,
Cleveland, Ohio.

APPENDIX A

SYMBOLS

The following symbols are used in this report:

c_p	specific heat, Btu/(lb)($^\circ$R)
h	height of tunnel, 10 in.
K	power factor = $\frac{\text{total calculated power}}{\text{theoretical normal shock power}}$
l	distance from initial wall-pressure rise to subsonic-diffuser inlet, in.
M	test-section Mach number
M_e	effective Mach number at subsonic-diffuser inlet
P	total pressure, in. mercury absolute
P_a,P_b	total pressure ahead of and behind the normal shock, in. mercury absolute
p	static pressure, in. mercury absolute
P_1,P_2	initial and final pressures
T_1	initial total temperature of air, $^\circ$R
W_b	weight flow of air bled, lb/sec
W_T	total weight of air passing through tunnel, lb/sec
x	distance from vertical center line
x_w	distance from vertical center line to wall, 1.92 in.
y	distance from horizontal center line
y_w	distance from horizontal center line, to wall, 5 in.

γ ratio of specific heats, 1.4

Subscripts:

0 conditions in settling chamber

3 conditions at subsonic-diffuser inlet

4 conditions at subsonic-diffuser outlet

APPENDIX B

DEFINITION OF POWER FACTOR

The rate of work, or power absorbed, by pumping a gas between two stations may be defined by the isentropic enthalpy change between the two stations. Thus,

$$\text{Power}\left(\frac{\text{Btu}}{\text{sec}}\right) = W_T c_p T_1 \left[\left(\frac{p_2}{p_1}\right)^{\frac{\gamma-1}{\gamma}} - 1\right] \tag{1}$$

where $p_2 > p_1$. When the flow follows several paths, the power required can be defined as the sum of the individual powers. Then

$$\text{Power} = c_p T_1 \sum_{n=1}^{N} w_n \left[\left(\frac{p_{2,n}}{p_{1,n}}\right)^{\frac{\gamma-1}{\gamma}} - 1\right] \tag{2}$$

For a supersonic wind tunnel with given test-section size, the Mach number and the inlet conditions W_T and T_1 are known and a theoretical normal shock total-pressure ratio P_0/P_1 is defined. Then the theoretical normal-shock power can be written

$$\text{Normal shock power} = W_T c_p T_1 \left[\left(\frac{P_a}{P_b}\right)^{\frac{\gamma-1}{\gamma}} - 1\right] \tag{3}$$

where

P_a total pressure ahead of normal shock

P_b total pressure behind normal shock

A nondimensional power factor, defined as the ratio of the calculated actual power to the theoretical normal-shock power, can then be expressed as follows:

$$K = \frac{\text{Power}}{\text{Normal shock power}} = \frac{c_p T_1 \sum_{n=1}^{N} w_n \left[\left(\frac{p_{2,n}}{p_{1,n}} \right)^{\frac{\gamma-1}{\gamma}} - 1 \right]}{W_T c_p T_1 \left[\left(\frac{p_a}{p_b} \right)^{\frac{\gamma-1}{\gamma}} - 1 \right]} \qquad (4)$$

which can be rewritten as

$$K = \frac{\sum_{n=1}^{N} \left(\frac{w_n}{W_T} \right) \left[\left(\frac{p_{2,n}}{p_{1,n}} \right)^{\frac{\gamma-1}{\gamma}} - 1 \right]}{\left[\left(\frac{p_a}{p_b} \right)^{\frac{\gamma-1}{\gamma}} - 1 \right]} \qquad (5)$$

Equation (5) is the power factor used in this report. The numerator may be separated into internal power and bleed power for ease of identification, which gives

$$K = \frac{\left[\left(\frac{p_0}{p_4} \right)^{\frac{\gamma-1}{\gamma}} - 1 \right] + \sum_{n=1}^{N} \frac{w_n}{W_T} \left[\left(\frac{p_{2,n}}{p_{1,n}} \right)^{\frac{\gamma-1}{\gamma}} - 1 \right]}{\left[\left(\frac{p_a}{p_b} \right)^{\frac{\gamma-1}{\gamma}} - 1 \right]} \qquad (6)$$

where the summation in the numerator now represents the portion of the power factor required for the bleed process.

For the evaluation of power factor in this report, $p_{1,n}$ was taken as the measured pressures in the individual 1-inch suction tubes and $p_{2,n}$ was taken as the recovered total pressure P_4. Thus it was assumed that the bled weight flow was pumped from the measured static pressure to station 4.

REFERENCE

1. Neumann, E. P., and Lustwerk, F.: Supersonic Diffusers for Wind Tunnels. Jour. Applied Mech., vol. 16, no. 2, June 1949, pp. 195-202.

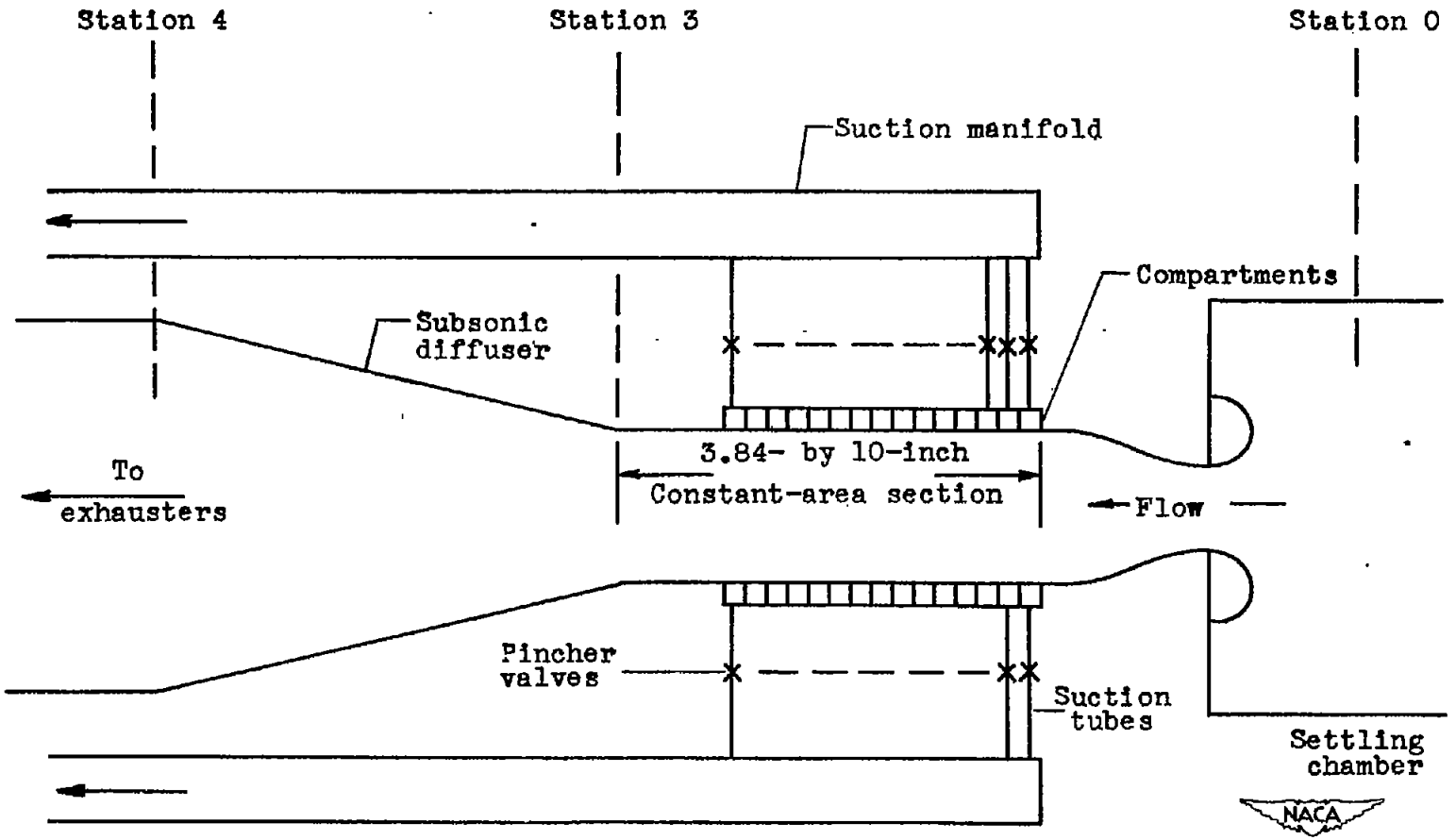

(a) Schematic diagram of installation.

Figure 1. - Boundary-layer-suction installation in 3.84- by 10-inch tunnel.

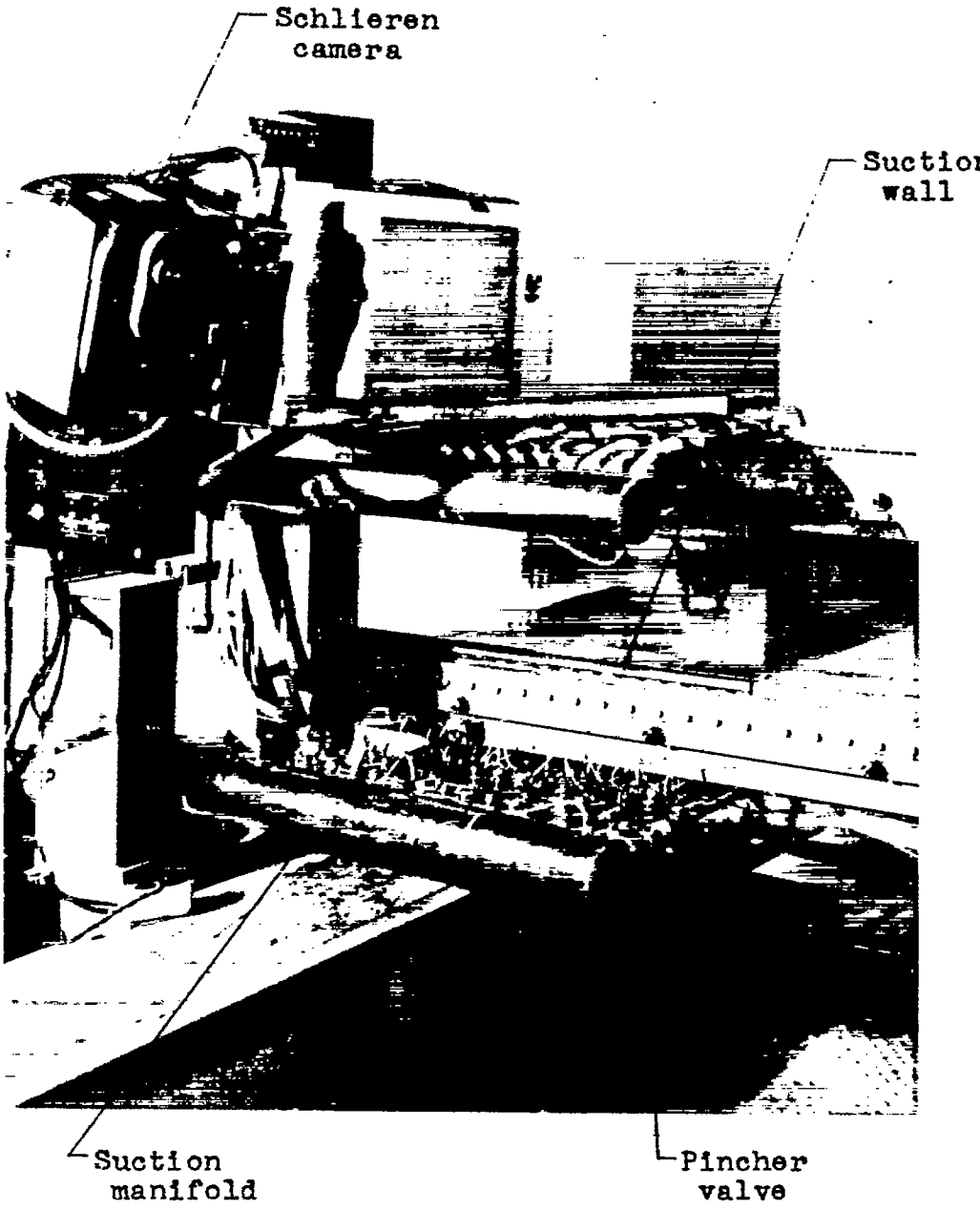

(b) Photograph of installation.

C-23013

Figure 1. - Concluded. Boundary-layer-suction installation in 3.84- by 10-inch tunnel.

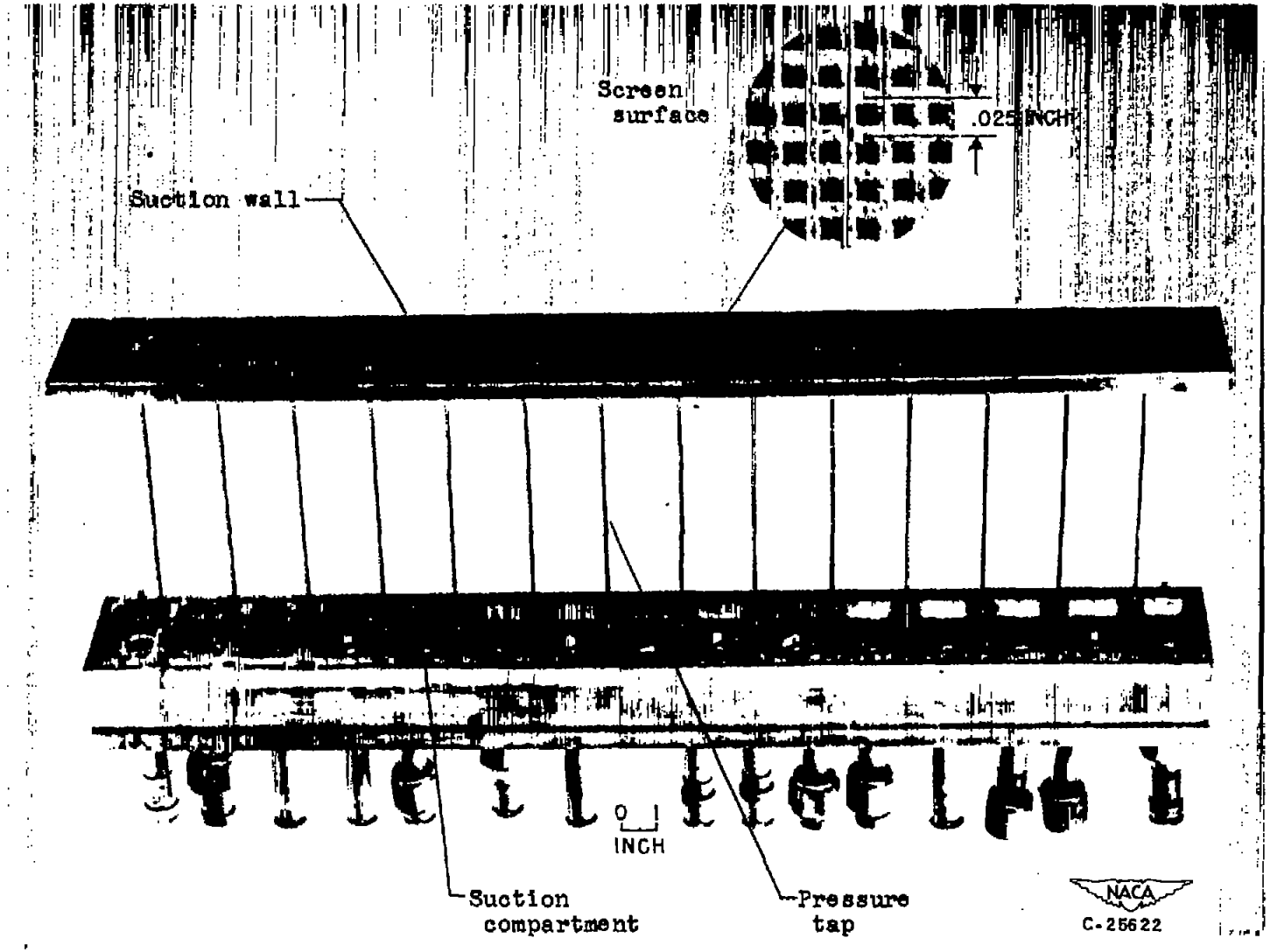

Figure 2. - Suction-wall assembly of 3.84- by 10-inch tunnel. (Suction wall raised to show compartments.)

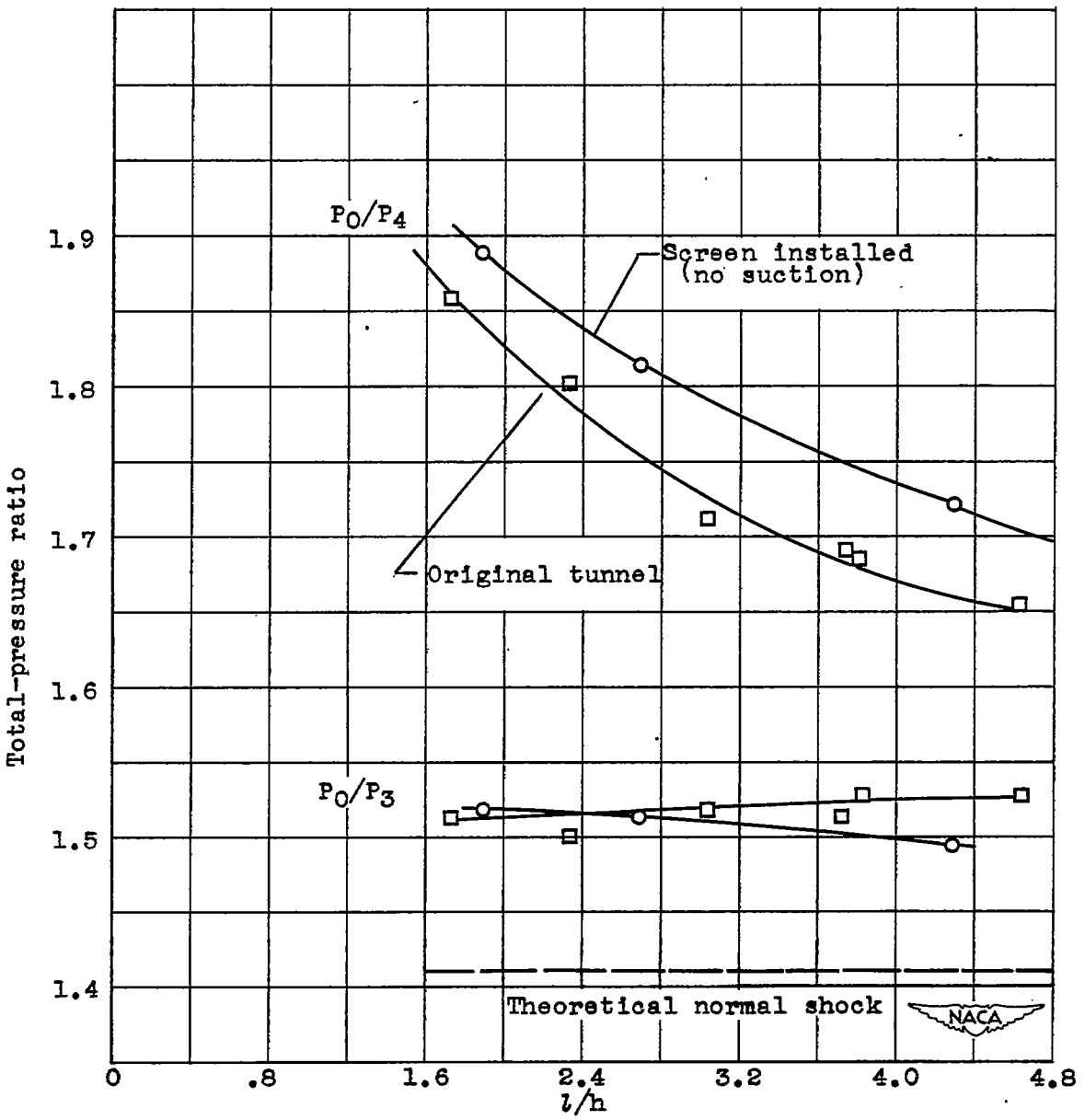

Figure 3. - Effect of screen installation on total-pressure ratios.

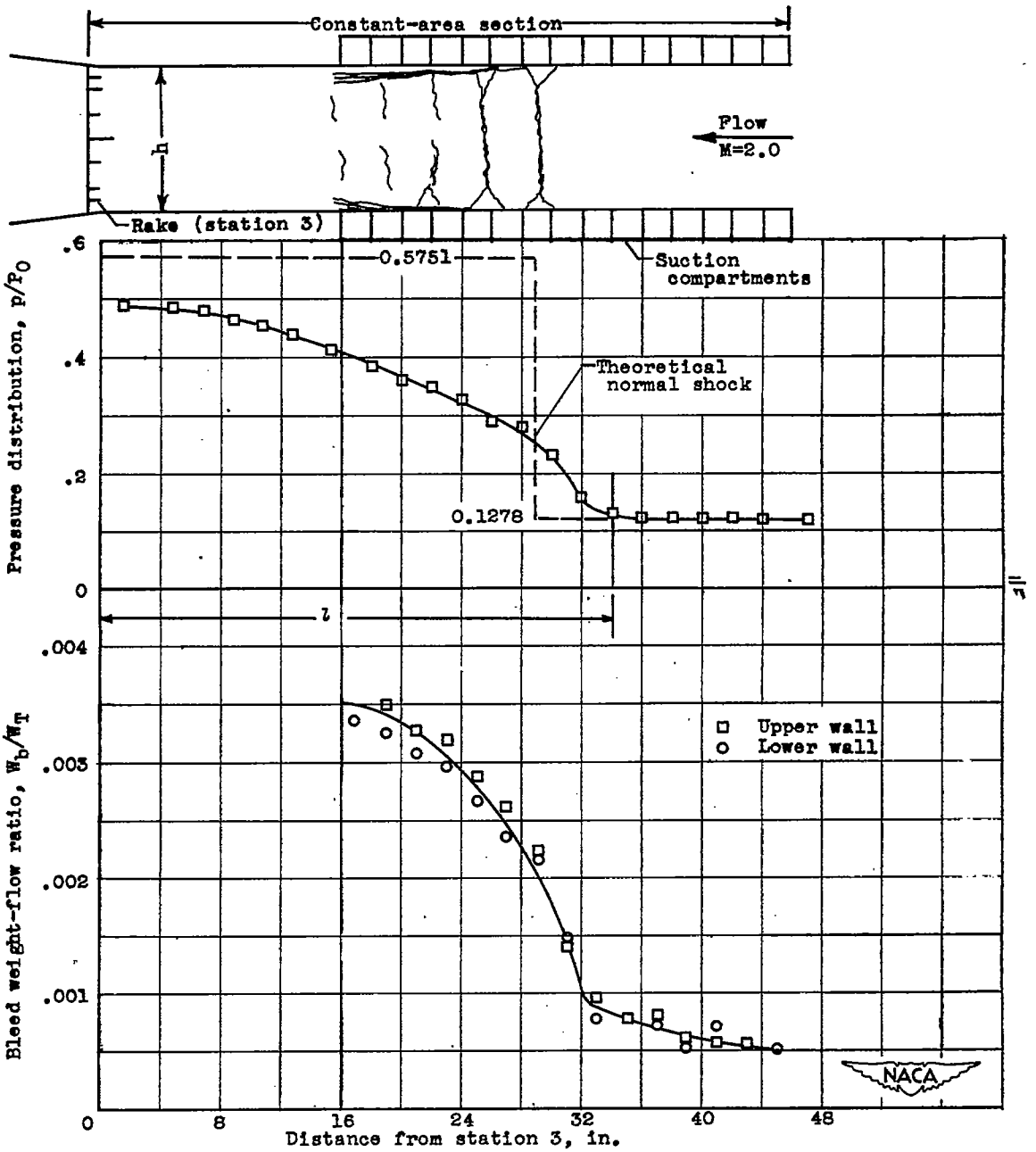

Figure 4. - Data from typical reading.

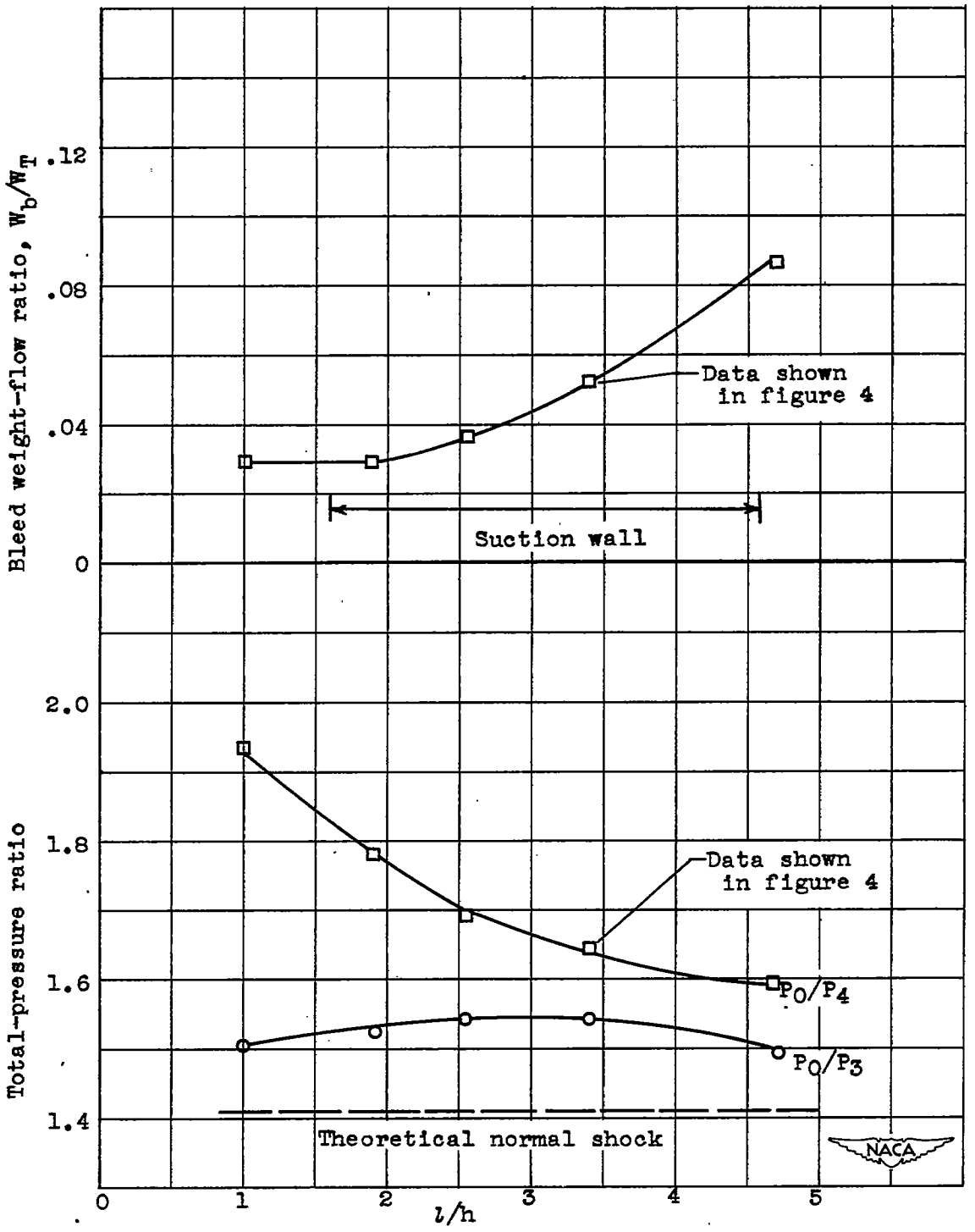

Figure 5. - Typical variation of bleed weight-flow ratio and pressure ratios with shock position.

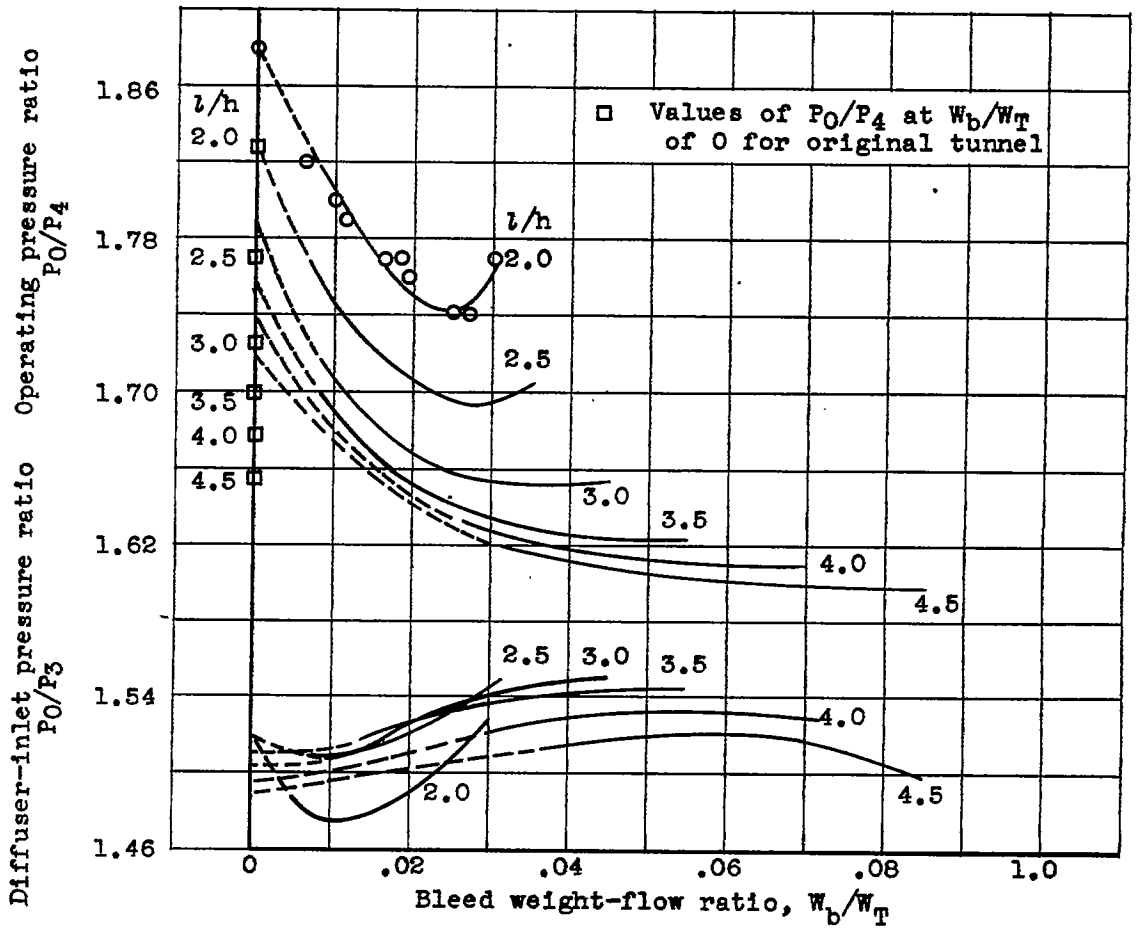

(a) Variation of P_0/P_4 and P_0/P_3 with W_b/W_T for several values of l/h.

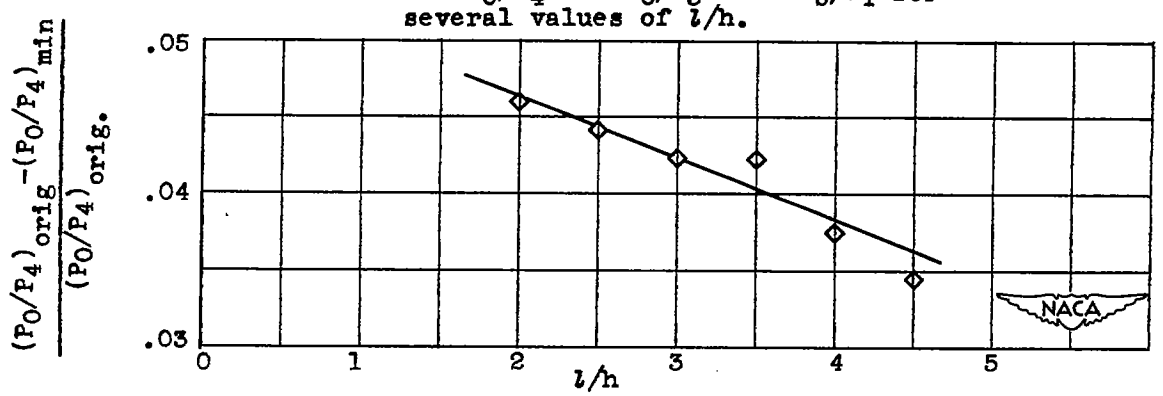

(b) Variation of percent reduction of P_0/P_4 with l/h.

Figure 6. - Effect of boundary-layer suction on total-pressure ratios.

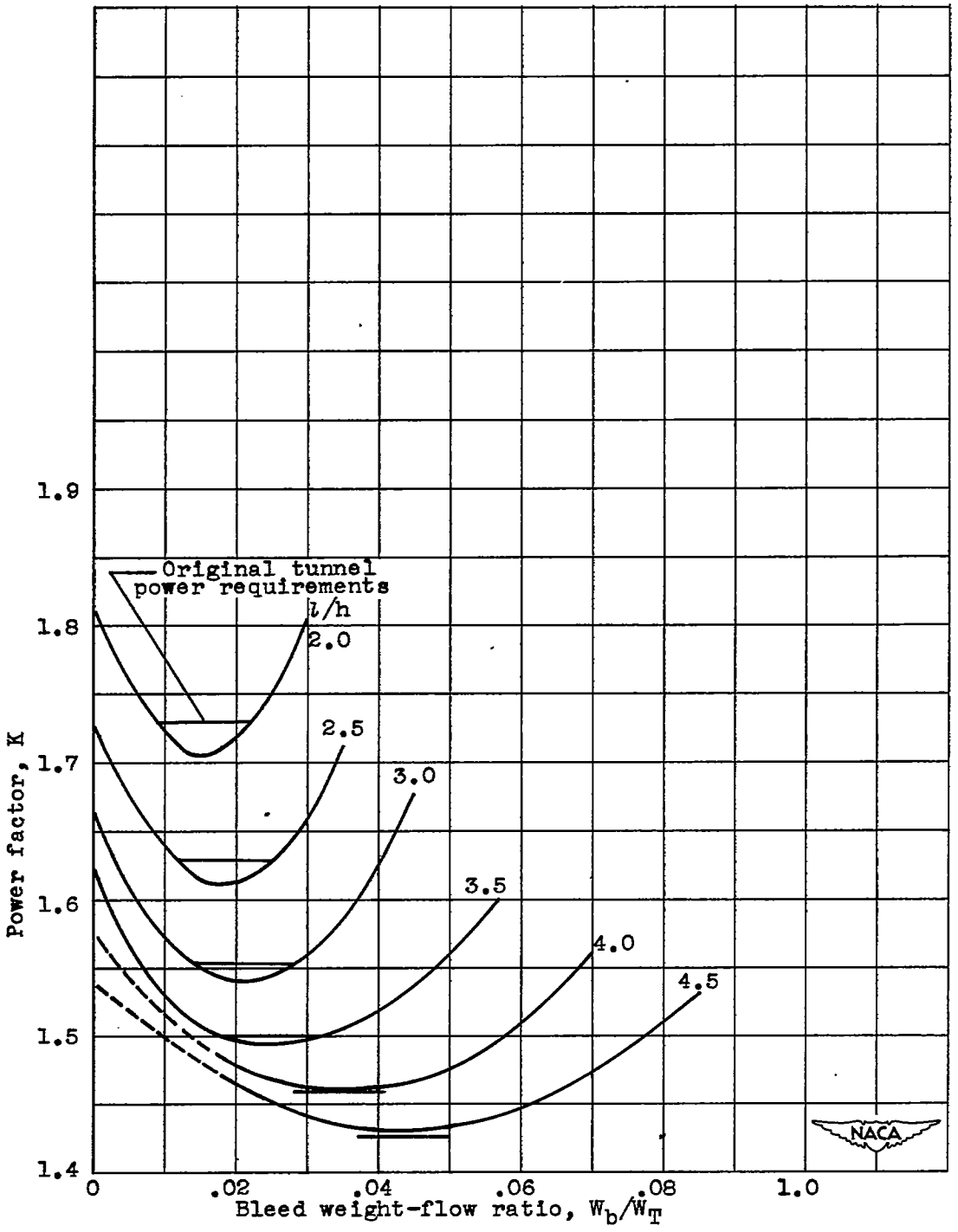

(a) Over-all power factor.

Figure 7. - Variation of power factor with bleed weight-flow ratio.

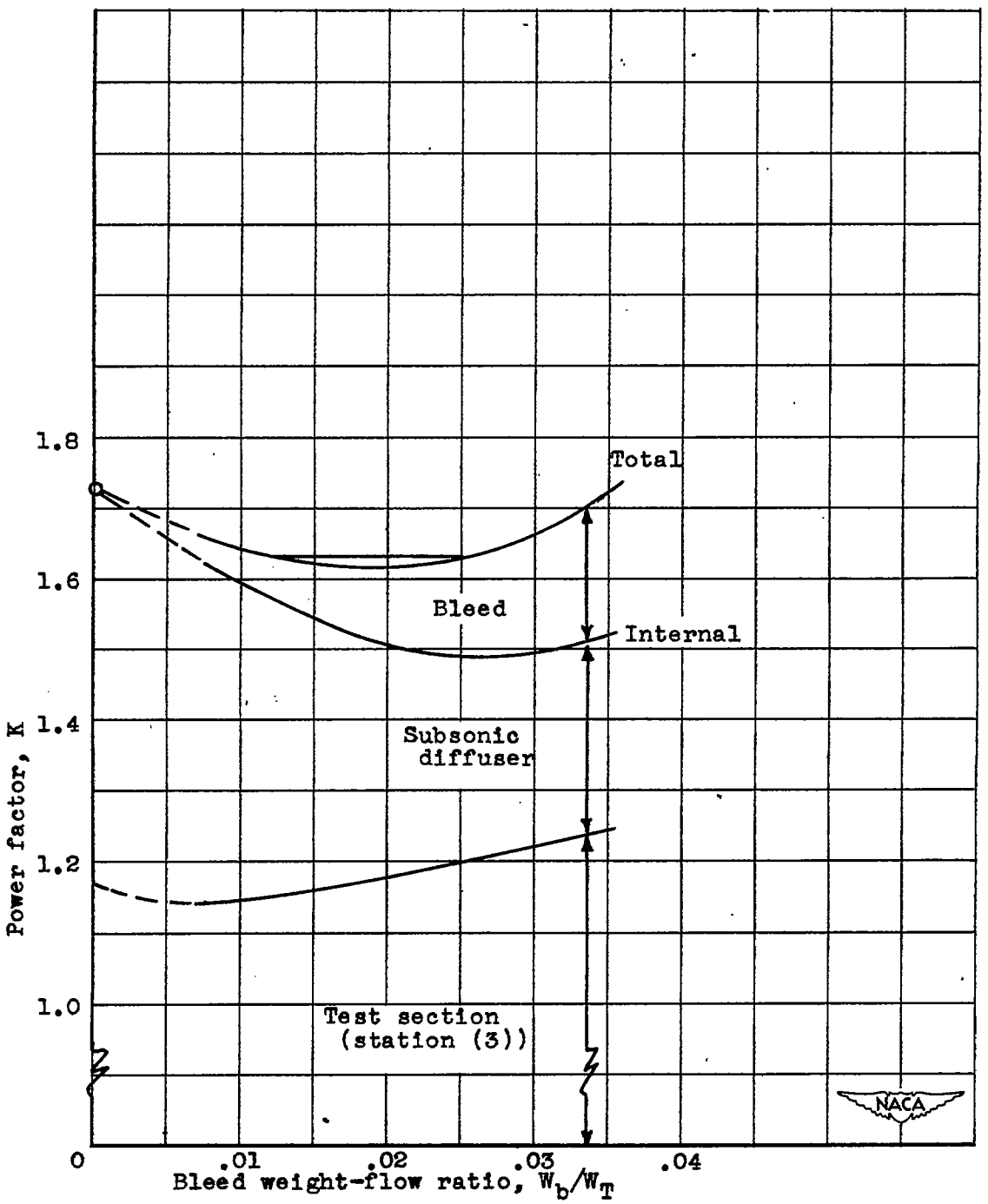

(b) Component breakdown of power factor for l/h of 2.5.

Figure 7. - Concluded. Variation of power factor with bleed weight-flow ratio.

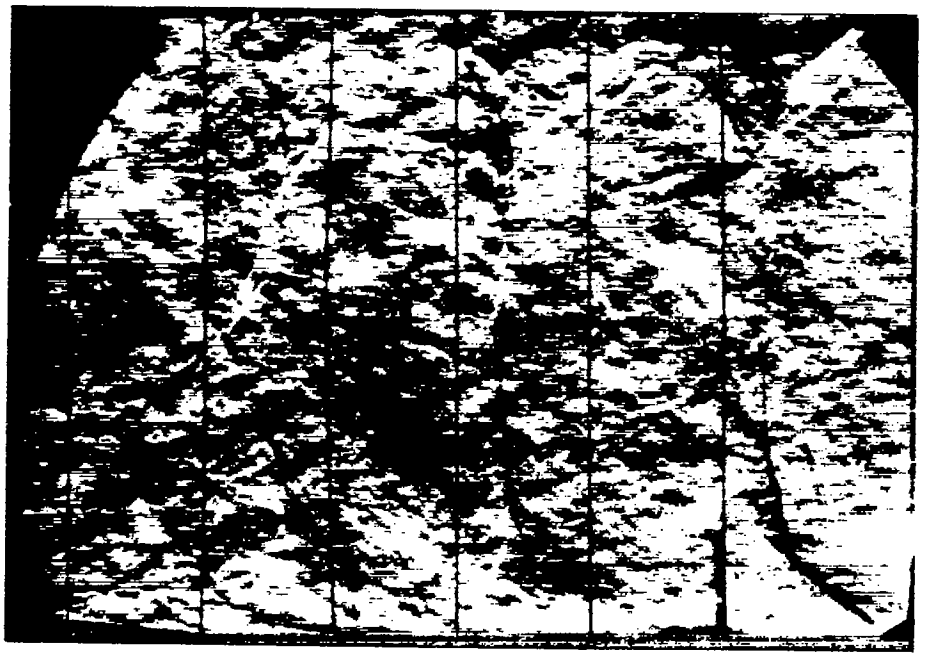

Bleed weight-flow ratio, $W_b/W_T \sim 0.109$

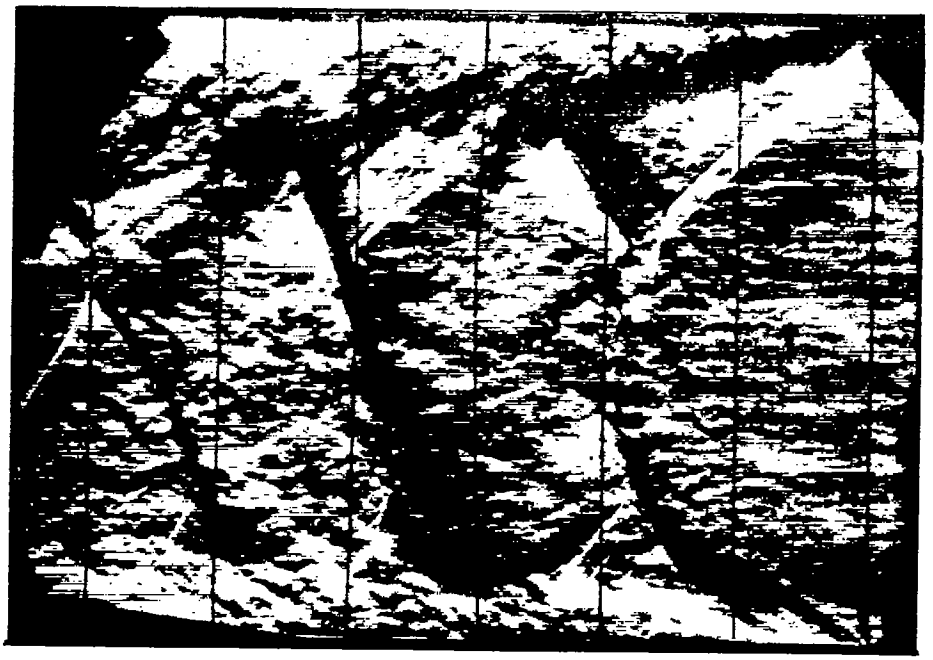

Bleed weight-flow ratio, $W_b/W_T = 0$ (screen installed)

(a) $l/h \sim 4.6$.

NACA

C-25621

Figure 8. – Schlieren photographs of terminal-shock configuration with and without boundary-layer suction. Exposure, 4 microseconds.

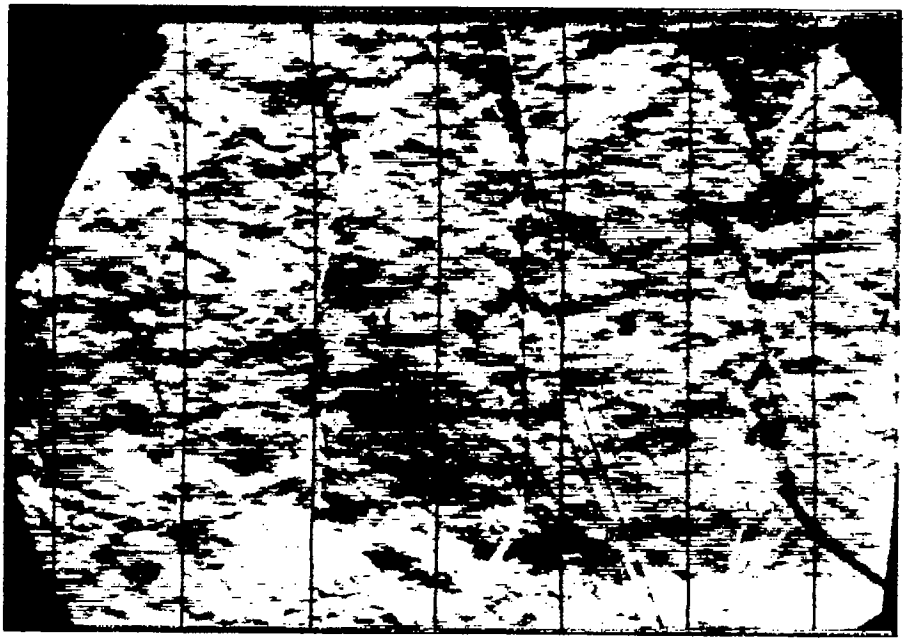

Bleed weight-flow ratio, $W_b/W_T \sim 0.057$

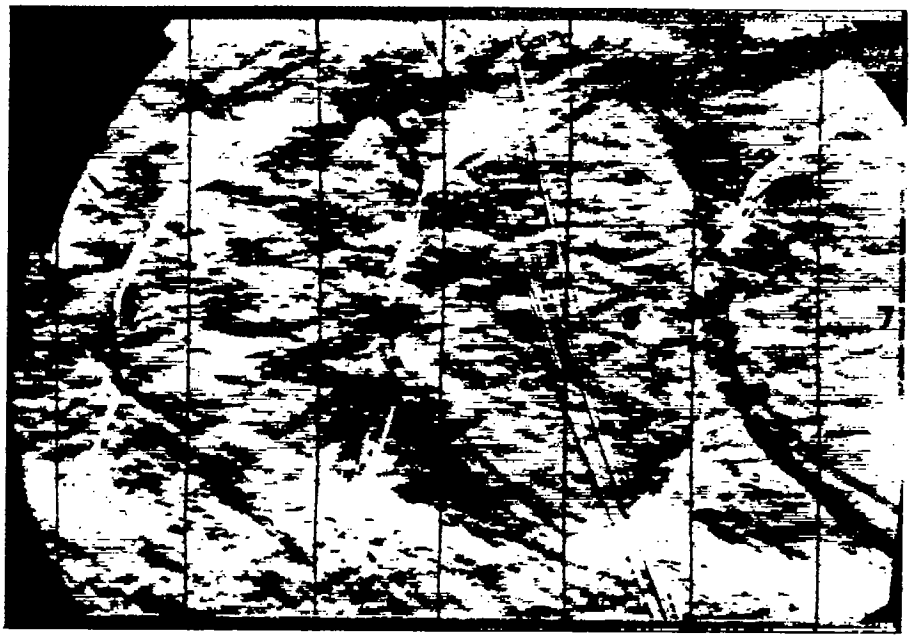

Bleed weight-flow ratio, $W_b/W_T = 0$ (screen installed)

(b) $l/h \sim 3.4$.

NACA

C-25620

Figure 8. - Continued. Schlieren photographs of terminal-shock configuration with and without boundary-layer suction. Exposure, 4 microseconds.

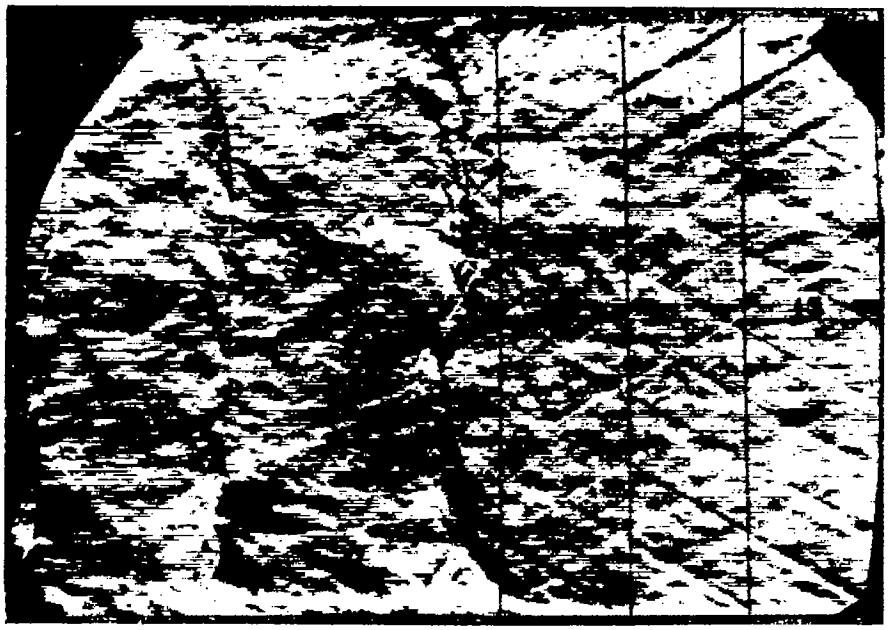

Bleed weight-flow ratio, $W_b/W_T \sim 0.027$

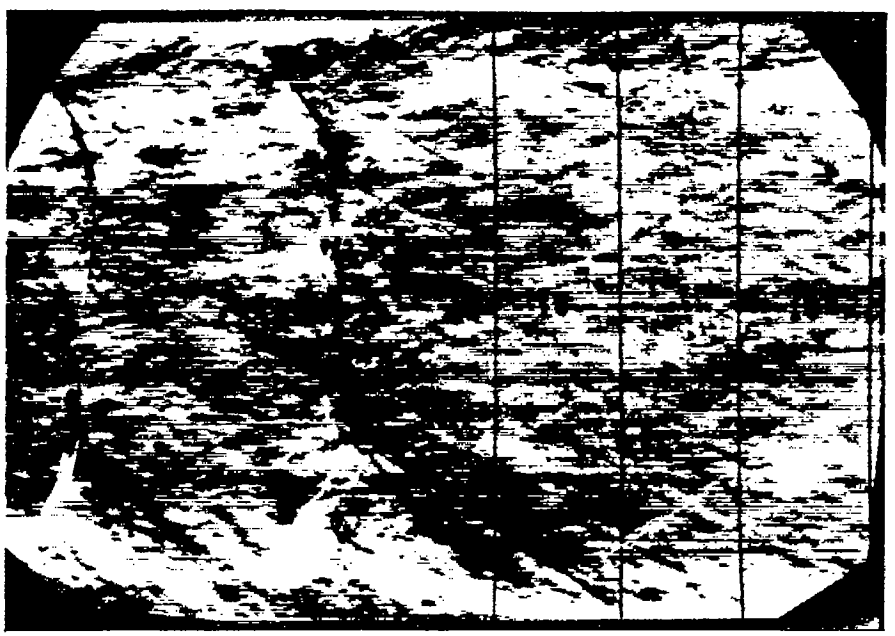

Bleed weight-flow ratio, $W_b/W_T = 0$ (screen installed)

(c) $l/h \sim 1.7$.

NACA

C-26005

Figure 8. - Continued. Schlieren photographs of terminal-shock configuration with and without boundary-layer suction. Exposure, 4 microseconds.

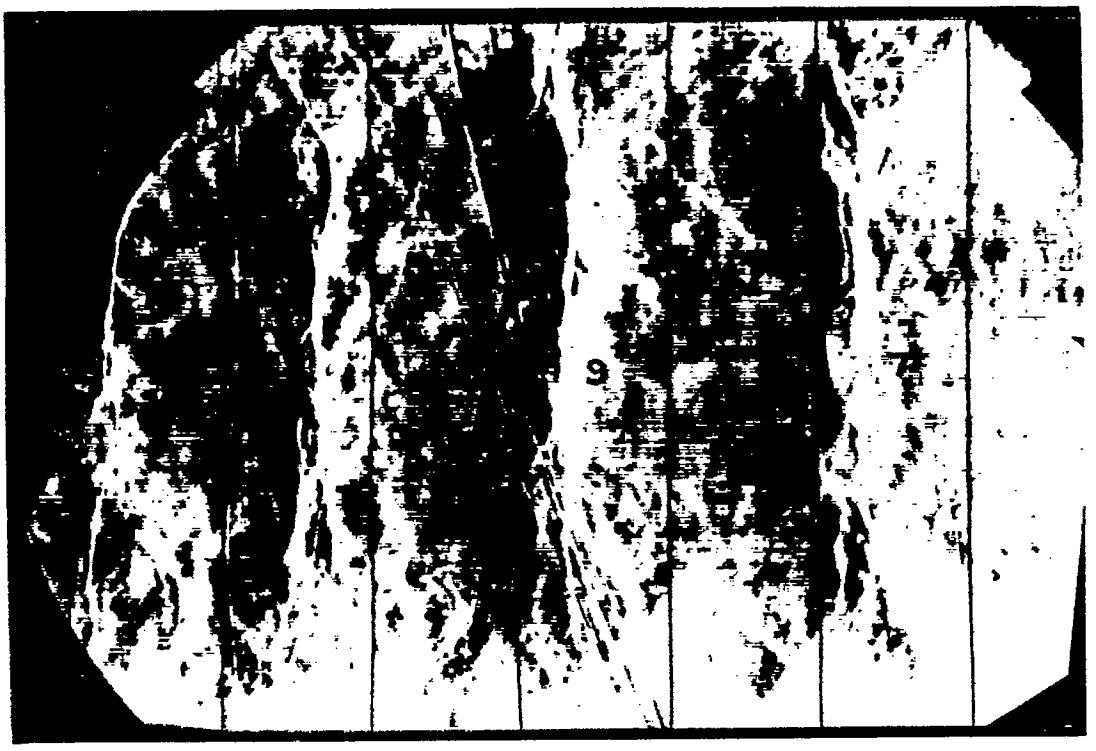

Knife edge vertical (suction applied)

(d) $l/h \sim 3.4$.

NACA C-26006

Figure 8. - Concluded. Schlieren photographs of terminal-shock configuration with and without boundary-layer suction. Exposure, 4 microseconds.

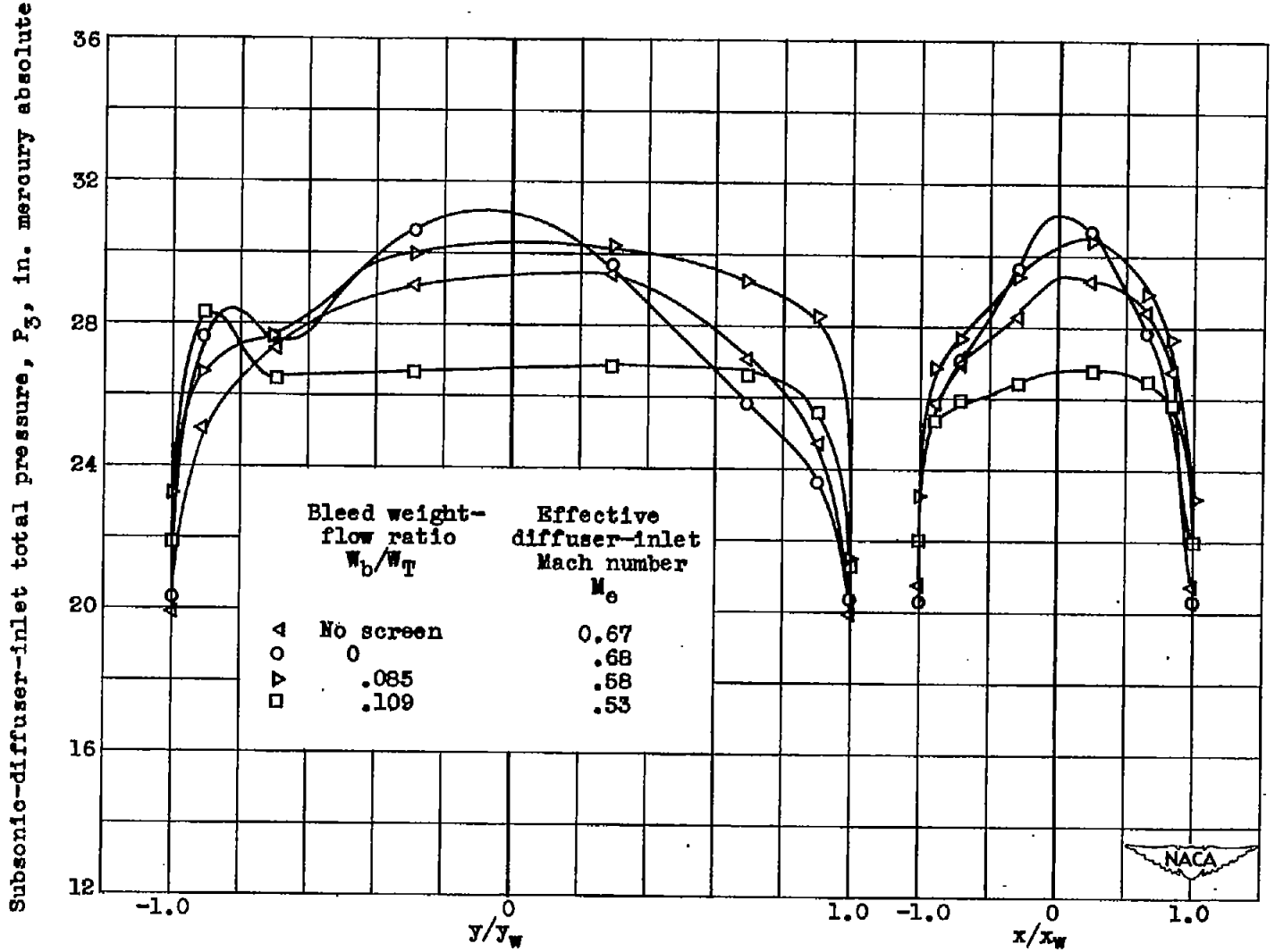

(a) $l/h \sim 4.7$.

Figure 9. - Total-pressure profiles at subsonic-diffuser inlet.

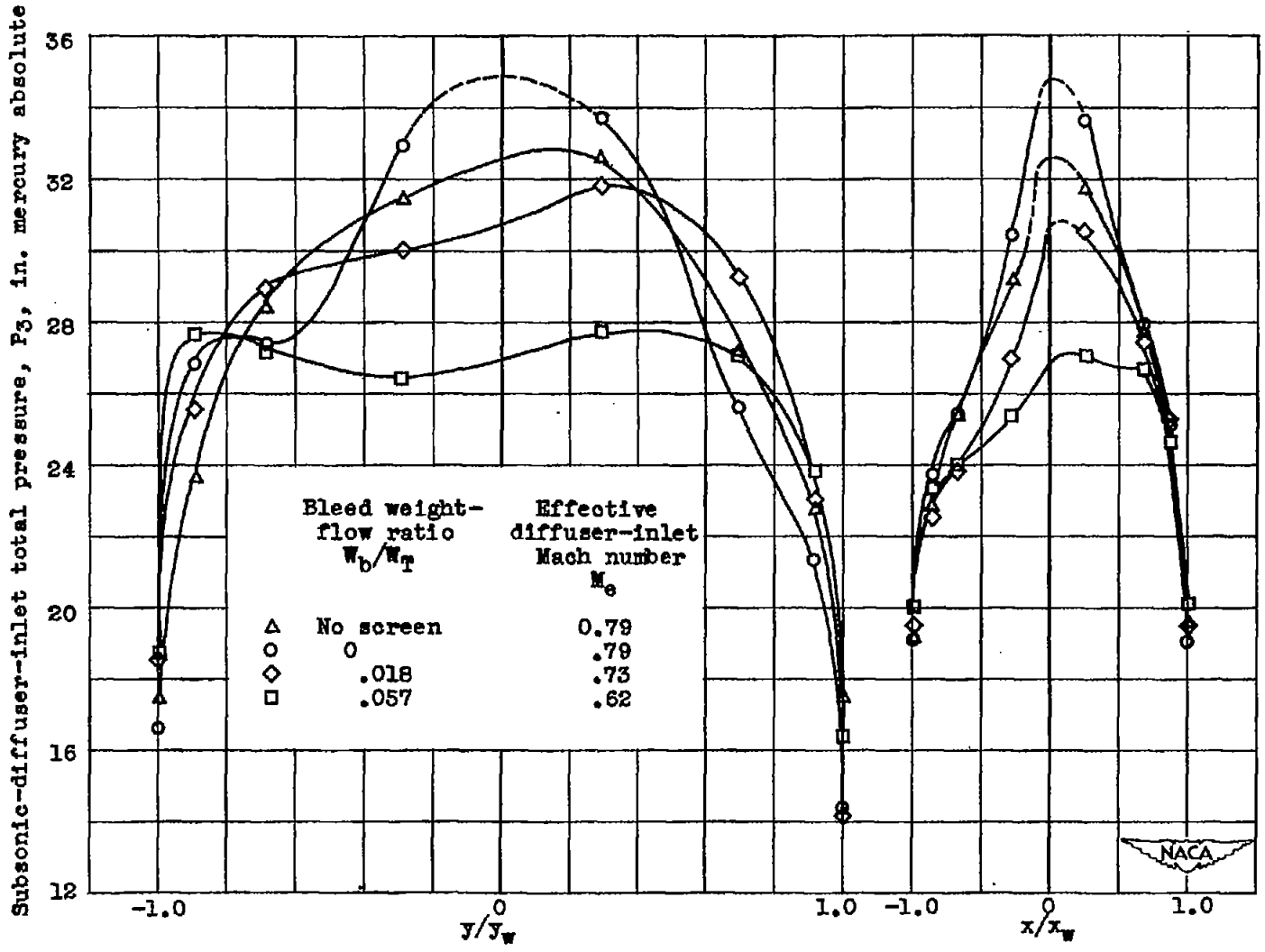

(b) $l/h \sim 3.4$.

Figure 9. - Continued. Total-pressure profiles at subsonic-diffuser inlet.

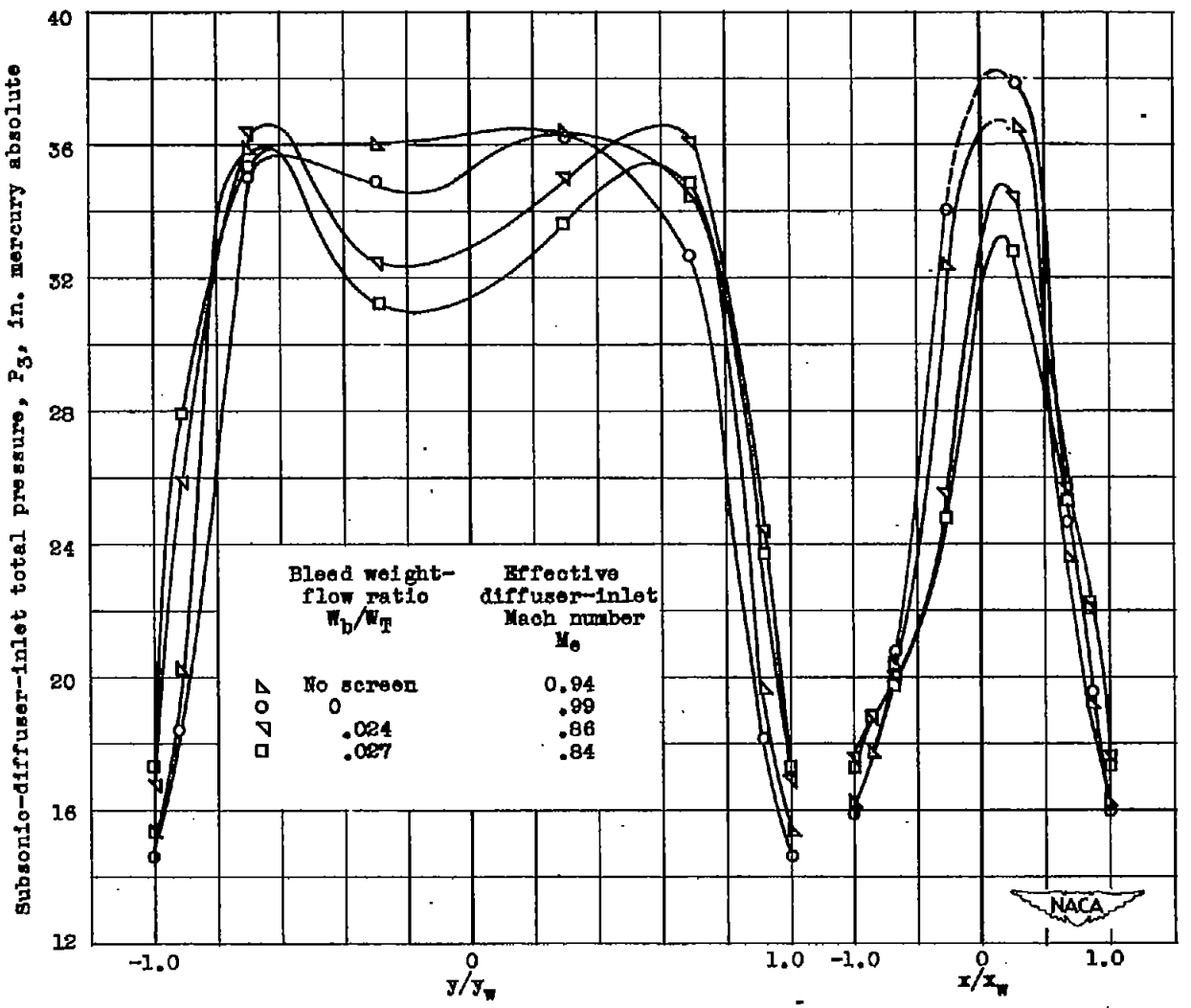

(c) $l/h \sim 1.7$.

Figure 9. - Concluded. Total-pressure profiles at subsonic-diffuser inlet.

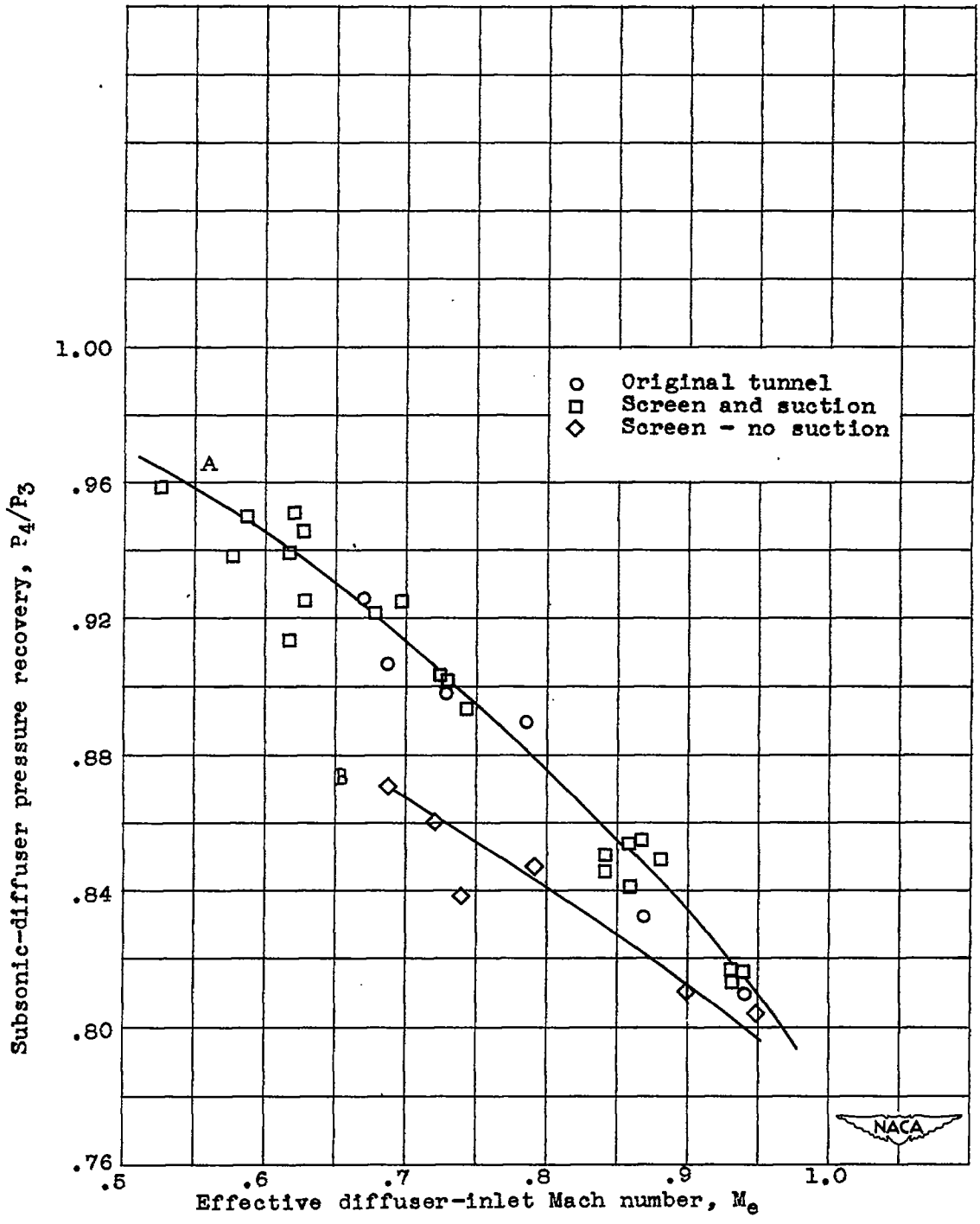

Figure 10. - Variation of subsonic-diffuser pressure recovery with effective diffuser-inlet Mach number.

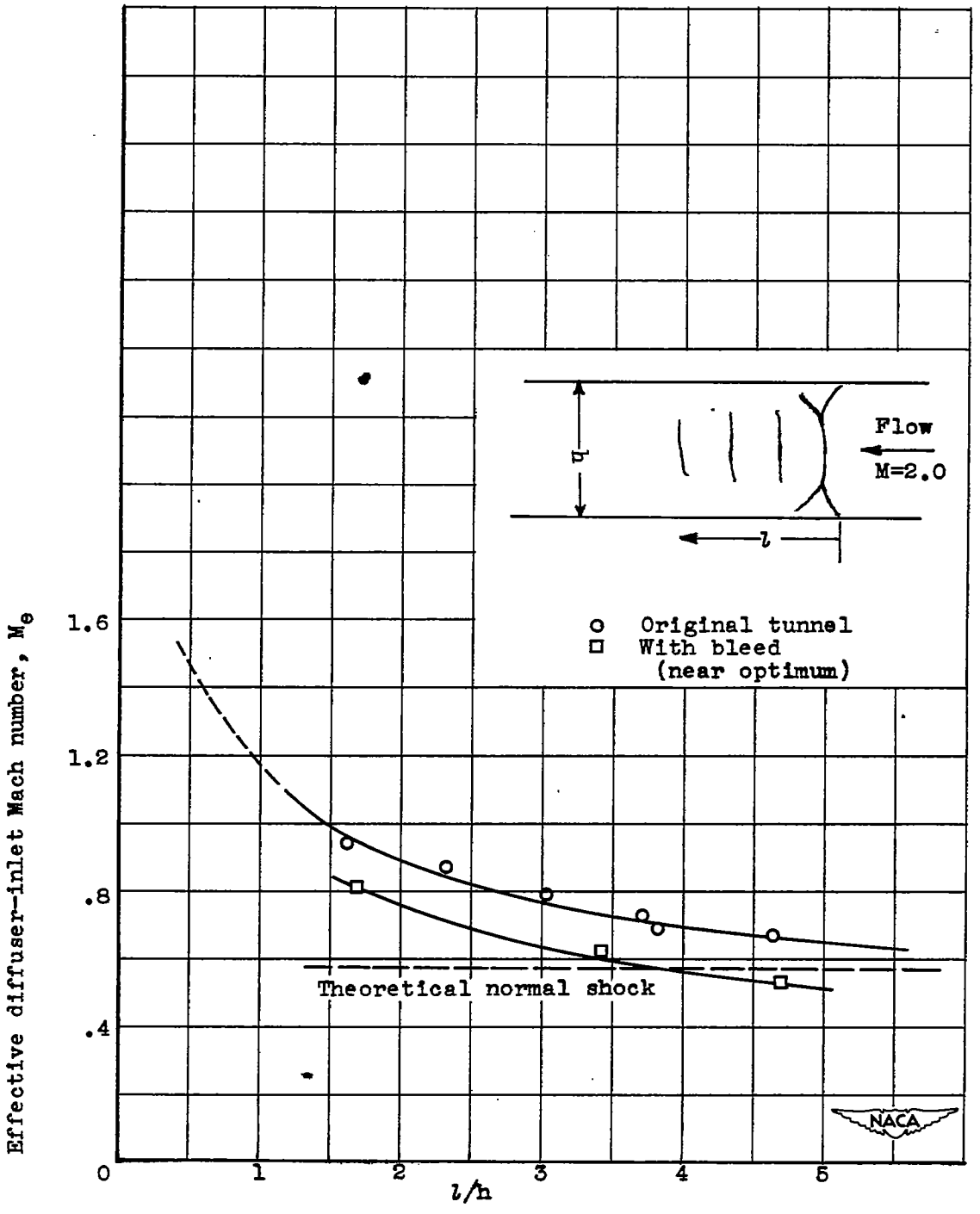

Figure 11. - Variation of effective diffuser-inlet Mach number with distance behind normal shock.